

# The $\rho \rightarrow \gamma\pi$ and $\omega \rightarrow \gamma\pi$ decays in quark-model approach and estimation of coupling for pion emission by quark

A V Anisovich, V V Anisovich, L G Dakhno, M A Matveev,  
V A Nikonov and A V Sarantsev

Petersburg Nuclear Physics Institute, 188300, Gatchina, Russia

**Abstract.** In the framework of the relativistic and gauge invariant spectral integral technique, we calculate radiative decays  $\rho(770) \rightarrow \gamma\pi(140)$  and  $\omega(780) \rightarrow \gamma\pi(140)$  supposing all mesons ( $\pi$ ,  $\rho$  and  $\omega$ ) to be quark–antiquark states. The  $q\bar{q}$  wave functions found for mesons and photon lead to a reasonably good description of data ( $\Gamma_{\rho^\pm \rightarrow \gamma\pi^\pm}^{(exp)} = 68 \pm 30$  keV,  $\Gamma_{\rho^0 \rightarrow \gamma\pi^0}^{(exp)} = 77 \pm 28$  keV,  $\Gamma_{\omega \rightarrow \gamma\pi^0}^{(exp)} = 776 \pm 45$  keV) that makes it possible to estimate the coupling for the bremsstrahlung emission of pion by quarks  $g_\pi \equiv g_\pi(u \rightarrow d\pi)$ . We have found two values for the pion bremsstrahlung coupling:  $|g_\pi| = 16.7 \pm 0.3 \begin{smallmatrix} +0.1 \\ -2.3 \end{smallmatrix}$  (Solution I) and  $|g_\pi| = 3.0 \pm 0.3 \begin{smallmatrix} +0.1 \\ -2.1 \end{smallmatrix}$  (Solution II). Within SU(6)-symmetry for nucleons, Solution I gives us for  $\pi NN$  coupling the value  $16.4 \leq g_{\pi NN}^2/(4\pi) \leq 23.2$  that is in qualitative agreement with the  $\pi N$  scattering data,  $g_{\pi NN}^2/(4\pi) \simeq 14$ . For excited states, we have estimated the partial widths in Solution I as follows:  $\Gamma(\rho_{2S}^\pm \rightarrow \gamma\pi) \simeq 10 - 130$  keV,  $\Gamma(\rho_{2S}^0 \rightarrow \gamma\pi) \simeq 10 - 130$  keV,  $\Gamma(\omega_{2S} \rightarrow \gamma\pi) \simeq 60 - 1080$  keV. The large uncertainties emphasise the necessity to carry out measurements of the meson radiative processes in the region of large masses.

PACS numbers: 12.39.Mk, 12.38.-t, 14.40.-n

Submitted to: *J. Phys. G: Nucl. Phys.*

## 1. Introduction

The radiative decay amplitude is a necessary element for the study of the quark–gluon structure of hadrons. In this paper, we present the calculation of the radiative decays of quark–antiquark states  $(q\bar{q})_{in} = \rho, \omega$  into  $\gamma\pi$ . In this way, we continue the calculations initiated in [1] where radiative transitions of quarkonium states  $(Q\bar{Q})_{in} \rightarrow \gamma(Q\bar{Q})_{out}$  were studied, with the production of massive outgoing states  $(Q\bar{Q})_{out}$ . Considering the production of the  $\gamma\pi$  system, a particular necessity is to take into account, together with the annihilation  $q\bar{q} \rightarrow \pi$ , an additional process of the bremsstrahlung type, namely,  $q \rightarrow q\pi$ .

We treat the meson decay amplitude as triangle diagram of constituent quarks (additive quark model) calculated in terms of the spectral integration technique, see [2] and references therein. The spectral integral technique is rather profitable for the description of composite particles, for the content of a composite system is thus strictly controlled. Besides, this technique is rather convenient for the description of high spin states.

The equation for the composite  $q\bar{q}$  systems in the spectral integration technique was suggested in [3], it is a direct generalisation of the dispersion  $N/D$  equation [4] when the  $N$ -function was represented as an infinite sum of separable vertices, see [2] for detail. In terms of this equation, the  $b\bar{b}$  and  $c\bar{c}$  quarkonia were considered in [5], while the light-quark  $q\bar{q}$  mesons were studied in [6].

In [6], the levels of the one-component  $q\bar{q}$  systems (with  $I = 1$  or  $I = 0$  which are almost pure  $s\bar{s}$  or  $n\bar{n} = (u\bar{u} + d\bar{d})/\sqrt{2}$  states) were reconstructed as well as their wave functions. The  $q\bar{q}$  systems are formed at distances, where perturbative QCD does not work ( $r \sim 0.5 - 1.0$  fm). In this region (the region of soft interactions), we deal with constituent quarks and effective massive gluons (with mass of the order of 700–1000 MeV [7, 8, 9, 10, 11]). It means that quark–antiquark interactions undergone a significant changes as compared to small distances; besides, at large distances the confinement forces work. Therefore, interactions in the soft region should be reconstructed on the basis of experimental studies – in [6], the  $q\bar{q}$  interaction was reconstructed on the basis of available data for  $q\bar{q}$ -levels and the  $q\bar{q}$ -meson radiative decays.

The standard way to investigate quark–antiquark systems is to apply the Bethe–Salpeter equation [12] written in terms of Feynman integrals. One may find the examples of such a study of light quark–antiquark systems in [13, 14, 15, 16, 17] and for heavy quarkonia ( $c\bar{c}$  and  $b\bar{b}$ ) in [17, 18, 19, 20, 21, 22], see also references therein.

However, one should keep in mind an important difference between the standard Bethe–Salpeter equation and that written in terms of the spectral integral [3]. In the dispersion relation technique, the constituents in the intermediate state are mass-on-shell,  $k_i^2 = m^2$ , while in the Feynman technique, which is used in the Bethe–Salpeter equation,  $k_i^2 \neq m^2$ . So, in the spectral integral equation, when the high spin state structures are calculated, we have a numerical factor  $k_i^2 = m^2$ , while in the Feynman technique one should write  $k_i^2 = m^2 + (k_i^2 - m^2)$ . Here, the first term in the right-

hand side provides us the contribution similar to that used in the spectral integration technique, while the second term cancels one of denominators of the kernel of the Bethe–Salpeter equation, that results in the penguin or tadpole type diagrams – let us call them zoo-diagrams. A particular property of the spectral integral technique is the exclusion of zoo-diagrams from the equation for composite systems.

The spectral integral equation [3] gives us a unique solution for the quark–antiquark levels and their wave functions, provided the interquark interaction is known. Let us emphasize that the equation works for both instantaneous interactions and the  $t$ -channel exchanges with retardation, and even for the energy-dependent interactions: this follows from the fact that the equation itself is the modified dispersion relation for the amplitude. For solving the inverse problem, that is, for reconstructing the interaction, it is not enough to know the meson masses — one should know wave functions of quark–antiquark systems. Such an information is contained in the hadronic form factors and radiative decay amplitudes. Therefore, in the approach of refs. [3, 5, 6], we consider simultaneously the meson levels in terms of the spectral integral equations and the meson radiative transitions in terms of the double dispersion relations over  $q\bar{q}$  states (or over corresponding meson masses) — in this way all calculations are carried out within compatible methods.

The calculation of radiative transition amplitudes in terms of the double dispersive integrals was performed for some selected reactions in [23, 24, 25, 26, 27] — the basic points of the method of operator expansion used in the calculation of double dispersive integrals can be found in [1, 2, 28].

The analyses of the light  $q\bar{q}$  systems [6] and heavy  $Q\bar{Q}$  quarkonia [5] in terms of the spectral integral equation differ from one another in certain respect, because the available experimental data are of different sort: for the  $Q\bar{Q}$  systems the only known are low-lying states (with an exception for the  $1^{--}$  quarkonia  $\Upsilon$  and  $\psi$  where a long series of vector states was discovered in the  $e^+e^-$  annihilation). At the same time, for the low-lying states there exists a rich set of data on radiative decays:  $(Q\bar{Q})_{\text{in}} \rightarrow \gamma(Q\bar{Q})_{\text{out}}$  and  $(Q\bar{Q})_{\text{in}} \rightarrow \gamma\gamma$ . For the light quark sector ( $q\bar{q}$  systems), there exists an abundant information on masses of highly excited states with different  $J^{PC}$  (see [29, 30, 31, 32, 33] and surveys [2, 34, 35]), but the knowledge of radiative decays is rather poor.

Despite the scarcity of data on radiative decays, the light  $q\bar{q}$  states have been studied in [6], relying upon our knowledge of linear trajectories in the  $(n, M^2)$ -plane, where  $n$  is the radial quantum number of the  $q\bar{q}$ -meson with mass  $M$  (see [2, 36]). We hope that it may somehow compensate the lack of information on the wave functions. In the fitting procedure [6], the main attention was paid to the states with large masses, expecting to extract the confinement interaction. We obtained that the strong  $t$ -channel interaction (which, as we think, determines the confinement) should exist in both scalar  $I \otimes I$  and vector  $\gamma_\mu \otimes \gamma_\mu$  channels. The fitting results point rather reliably to the equality of these  $t$ -channel interactions [6].

Obviously, the fitting results presented in [6] should be checked (and, if necessary, improved) by investigating the other radiative decays – following to this program we

consider here the decays  $\rho \rightarrow \gamma\pi$  and  $\omega \rightarrow \gamma\pi$ . Small mass of the pion requires to take into account not only the process of photon emission with a subsequent quark–antiquark annihilation  $q\bar{q} \rightarrow \pi$  (triangle diagram of the additive quark model, Fig. 1) but also the bremsstrahlung-type emission of pion  $q \rightarrow \pi q$ , with subsequent quark–antiquark annihilation into photon  $q\bar{q} \rightarrow \gamma$ , see Fig. 2. Therefore, the key points in the calculation of the  $\rho, \omega \rightarrow \gamma\pi$  decays is to know  $q\bar{q}$  wave functions of pion and vector mesons ( $\rho$  and  $\omega$ ) as well as  $q\bar{q}$  wave function of the photon  $\gamma \rightarrow q\bar{q}$ . Also the fitting procedure calls us to determine the pion bremsstrahlung constant for the process  $q \rightarrow \pi q$ .

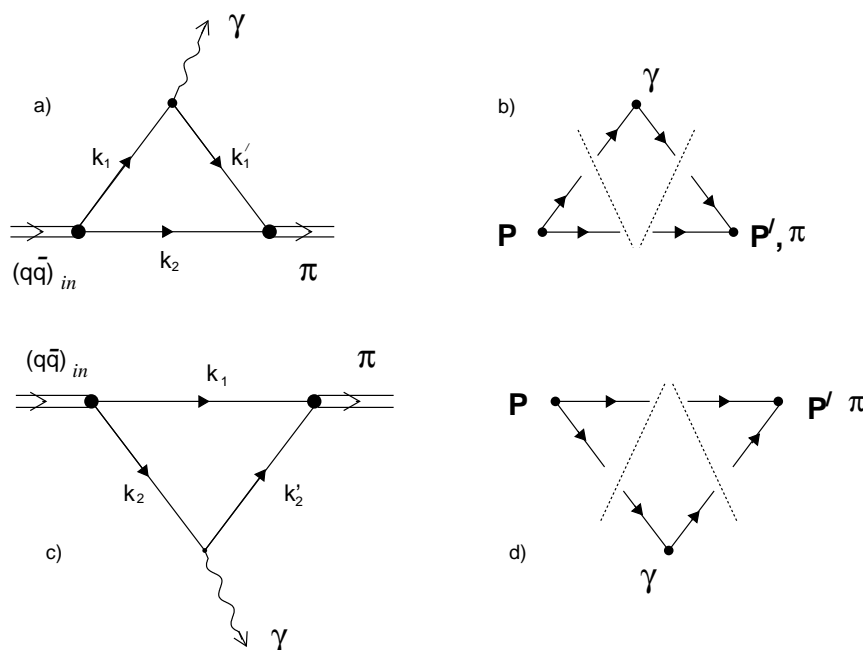


**Figure 1.** a), c) Triangle diagrams for radiative transition  $(q\bar{q})_{in} \rightarrow \gamma\pi$  with the emission of photon by quark; here  $p^2 = M_{in}^2$ ,  $p'^2 = M_\pi^2$  and  $(p - p')^2 = q^2$ . b), d) Cuttings of the triangle diagrams 1a and 1c signify the double discontinuity of the spectral integral with intermediate-state momentum squared  $P^2 = s$ ,  $P'^2 = s'$  and  $(P - P')^2 = q^2$ .

### 1.1. Photon wave function

For the region  $0 \lesssim Q^2 \lesssim 1$  (GeV/c)<sup>2</sup> (here  $Q^2 = -q^2$ ), the light-quark components of the photon wave function  $\gamma^*(Q^2) \rightarrow q\bar{q}$  ( $q = u, d, s$ ) are determined in [37] (see also [2]) on the basis of data for the transitions  $\pi^0, \eta, \eta' \rightarrow \gamma\gamma^*(Q^2)$  and reactions of  $e^+e^-$ -annihilation:  $e^+e^- \rightarrow \rho^0, \omega, \phi$  and  $e^+e^- \rightarrow hadrons$  at  $1 < E_{e^+e^-} < 3.7$  GeV (in a more rough approximation the wave function  $\gamma(Q^2) \rightarrow q\bar{q}$  was found in [38]).

Conventionally, one may consider two pieces of the photon wave function: soft and hard ones. Hard component relates to the point-like vertex  $\gamma \rightarrow q\bar{q}$ , it is responsible for the production of quark–antiquark pair at high virtuality. At high energies of the

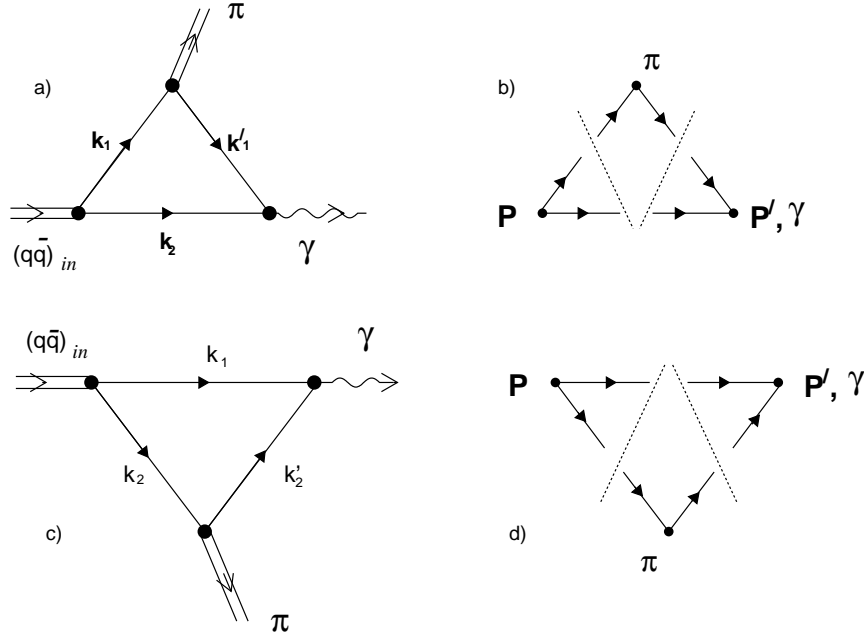


**Figure 2.** a), c) Triangle diagrams for radiative transition  $(q\bar{q})_{in} \rightarrow \gamma\pi$  with the emission of pion by quark; here  $p^2 = M_{in}^2$ ,  $p_\pi^2 = M_\pi^2$ . b), d) Cuttings of the triangle diagrams 2a and 2c for getting double discontinuity of the spectral integral with  $P^2 = s$ ,  $P'^2 = s'$  and  $(P - P')^2 = p_\pi^2$ .

$e^+e^-$  system, the ratio of cross sections  $R = \sigma(e^+e^- \rightarrow hadrons)/\sigma(e^+e^- \rightarrow \mu^+\mu^-)$  is determined by the hard component of photon wave function, while soft component is responsible for the production of low-energy quark-antiquark vector states such as  $\rho^0$ ,  $\omega$ ,  $\phi(1020)$ , and their excitations.

In the spectral integral technique, the quark wave function of the photon,  $\gamma^*(Q^2) \rightarrow q\bar{q}$ , is defined as follows:

$$\psi_{\gamma^*(Q^2) \rightarrow q\bar{q}}(s) = \frac{G_{\gamma \rightarrow q\bar{q}}(s)}{s + Q^2}, \quad (1)$$

where  $G_{\gamma \rightarrow q\bar{q}}(s)$  is the vertex for the transition of photon into  $q\bar{q}$  state, depending on the invariant energy squared,  $s$ , of  $q\bar{q}$  system. In terms of the light-cone variables  $s = (m^2 + k_\perp^2)/[x(1-x)]$ , where  $m$  is the quark mass,  $k_\perp$  and  $x$  are the light-cone characteristics of quarks: transverse momentum and a part of longitudinal momentum.

Rather schematically, the vertex function  $G_{\gamma \rightarrow q\bar{q}}(s)$  may be divided into two terms. The first term is responsible for the soft component which is due to the transition of photon to vector  $q\bar{q}$  meson  $\gamma \rightarrow V \rightarrow q\bar{q}$ , while the second one describes the point-like interaction in the hard domain. The principal characteristics of the soft component is the threshold value of the vertex and the rate of its decrease with energy. The hard component of the vertex is characterized by the energy where the point-like interaction becomes dominant.

In [38], the photon wave function has been found assuming the quark relative momentum dependence to be the same for all quark vertices:  $g_{\gamma \rightarrow u\bar{u}}(k^2) = g_{\gamma \rightarrow d\bar{d}}(k^2) = g_{\gamma \rightarrow s\bar{s}}(k^2)$ , where we redenoted  $G_{\gamma \rightarrow q\bar{q}}(s) \rightarrow g_{\gamma \rightarrow q\bar{q}}(k^2)$  with  $k^2 = s/4 - m^2$ . The hypothesis of the vertex universality for  $u$  and  $d$  quarks used in [37],

$$G_{\gamma \rightarrow u\bar{u}}(s) = G_{\gamma \rightarrow d\bar{d}}(s) \equiv G_\gamma(s) , \quad (2)$$

looks rather trustworthy because of the degeneracy of  $\rho$  and  $\omega$  states, though the similarity in the  $k$ -dependence for non-strange and strange quarks may be violated. Using experimental data on the transitions  $\gamma\gamma^*(Q^2) \rightarrow \pi^0, \eta, \eta'$  only, one cannot determine the parameters  $(C, b, s_0)$  – see below Eqs. (3) and (4) for both  $G_{\gamma \rightarrow s\bar{s}}(s)$  and  $G_\gamma(s)$ . We also add the  $e^+e^-$  annihilation data for the determination of wave functions, that is  $e^+e^- \rightarrow \gamma^* \rightarrow \rho^0, \omega, \phi(1020)$ , together with the ratio  $R(E_{e^+e^-}) = \sigma(e^+e^- \rightarrow \text{hadrons})/\sigma(e^+e^- \rightarrow \mu^+\mu^-)$  at  $E_{e^+e^-} > 1$  GeV. The reactions  $e^+e^- \rightarrow \gamma^* \rightarrow \rho^0, \omega, \phi(1020)$  are rather sensitive to the parameters  $C_a, b_a$ , while the data on  $R(E_{e^+e^-})$  allow us to fix the parameter  $s_0$ .

The transition vertices for  $u\bar{u}, d\bar{d} \rightarrow \gamma$  have been chosen in the form:

$$u\bar{u}, d\bar{d}: \quad G_\gamma(s) = c_\gamma \left( \exp(-b_1^\gamma s) + c_2^\gamma \exp(-b_2^\gamma s) \right) + \frac{1}{1 + e^{-b_0^\gamma (s-s_0^\gamma)}} \quad (3)$$

and the following parameter values have been found [2, 37]:

$$u\bar{u}, d\bar{d}: \quad c^\gamma = 32.506, \quad c_2^\gamma = -0.0187, \quad b_1^\gamma = 4 \text{ GeV}^{-2}, \quad b_2^\gamma = 0.8 \text{ GeV}^{-2}, \quad (4)$$

$$b_0^\gamma = 15 \text{ GeV}^{-2}, \quad s_0^\gamma = 1.614 \text{ GeV}^2 .$$

With these parameters, we have a good description of the available experimental data for  $V \rightarrow e^+e^-$  and two-photon decays, see [2, 6].

## 1.2. The $\rho$ , $\omega$ and $\pi$ wave functions

We characterise  $q\bar{q}$ -states by the following momentum-dependent wave functions:

$$\psi_n^{(S,L,J)}(k^2) = \frac{G_n^{(S,L,J)}(k^2)}{s - (M_n^{(S,L,J)})^2} , \quad (5)$$

where  $S, L, J$  are the spin, orbital momentum and total momentum of the  $q\bar{q}$  system with mass  $M_n^{(S,L,J)}$ .

*1.2.1.  $\rho(nL)$  and  $\omega(nL)$  states* We introduce spin-orbital operators and wave functions for the states with dominant  $L = 0, 2$  as follows:

$$\begin{array}{l|l|l} L = 0 & 0^{-+} & i\gamma_5 \psi_n^{(0,0,0)}(k^2) \\ \text{dominant } L = 0 & 1^{--} & \gamma_\mu^\perp \psi_n^{(1,0,1)}(k^2) \\ \text{dominant } L = 2 & 1^{--} & 3/\sqrt{2} \cdot \left( k_\mu^\perp \hat{k}^\perp - \frac{1}{3} k_\perp^2 \gamma_\mu^\perp \right) \psi_n^{(1,2,1)}(k^2). \end{array} \quad (6)$$

Here  $k^\perp$  is the relative quark–antiquark momentum,  $k_\mu^\perp = (g_{\mu\mu'} - P_\mu P_{\mu'}/P^2)k_{1\mu'} \equiv g_{\mu\mu'}^\perp k_{1\mu'} = -g_{\mu\mu'}^\perp k_{2\mu'}$ , so  $k^\perp \perp P = k_1 + k_2$ ; likewise,  $\gamma_\mu^\perp = g_{\mu\mu'}^\perp \gamma_{\mu'}$ . Definition of spin–momentum operators for other states can be found in [2, 28].

Generally, the states with different  $L$  mix with each other:

$$\begin{aligned}\hat{\psi}_\mu^{V(n,1)}(s) &= C_{10}^{(n)} \gamma_\mu^\perp \psi_n^{(1,0,1)}(k^2) + C_{12}^{(n)} \frac{3}{\sqrt{2}} \left( k_\mu^\perp \hat{k}^\perp - \frac{1}{3} k_\perp^2 \gamma_\mu^\perp \right) \psi_n^{(1,2,1)}(k^2), \\ \hat{\psi}_\mu^{V(n,2)}(s) &= C_{20}^{(n)} \gamma_\mu^\perp \psi_n^{(1,0,1)}(k^2) + C_{22}^{(n)} \frac{3}{\sqrt{2}} \left( k_\mu^\perp \hat{k}^\perp - \frac{1}{3} k_\perp^2 \gamma_\mu^\perp \right) \psi_n^{(1,2,1)}(k^2).\end{aligned}\quad (7)$$

But, according to [6], we have with a good accuracy  $C_{12}^{(n)} = C_{20}^{(n)} = 0$ , so below we put  $C_{10}^{(n)} = C_{22}^{(n)} = 1$ .

We parameterise the  $q\bar{q}$  wave functions of  $\rho$ ,  $\omega$  states,  $\psi_{(n)}^{(S,L,J)}(k^2)$ , with the following formula:

$$\psi_{(n)}^{(S,L,J)}(k^2) = e^{-\beta|k|^2} \sum_{i=1}^{11} c_i(S, L, J; n) |k|^{i-1}, \quad (8)$$

with cutting parameter  $\beta = 1.2 \text{ GeV}^{-2}$ . In Eq. (8), we use the notation  $|k| = \sqrt{s/4 - m^2}$  ( $m$  is the mass of the light constituent quark,  $m \simeq 350 \text{ MeV}$ ).

The constants  $c_i(S, L, J; n)$ , in GeV units, for mesons with  $L = 0$ ,  $\psi_n^{(S,L=0,J)}(k^2)$ , and  $L = 2$ ,  $\psi_n^{(S,L=2,J)}(k^2)$ , are presented in Eq. (9) and (10).

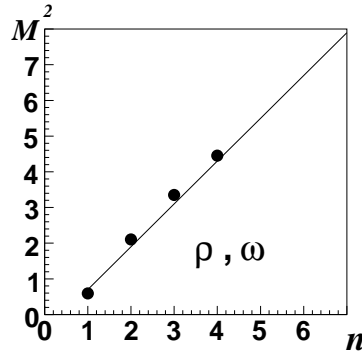


**Figure 3.** Trajectory for  $\rho_{nS}$  and  $\omega_{nS}$  states found in [6] ( $M_{\rho(nS)} = M_{\omega(nS)}$ ). Experimental values of the masses on  $\rho$ - and  $\omega$ -trajectories are equal to:  $[\rho_{1S}(775 \pm 10)$ ,  $\rho_{2S}(1460 \pm 20)$ ,  $\rho_{3S}(1870 \pm 70)$ ,  $\rho_{4S}(2110 \pm 35)]$  and  $[\omega_{1S}(782)$ ,  $\omega_{2S}(1430 \pm 50)$ ,  $\omega_{3S}(\sim 1830)$ ,  $\omega_{4S}(2205 \pm 40)]$ .

In the solution found in [6], the  $\rho_{nS}$  and  $\omega_{nS}$  mesons are degenerated:  $M_{\rho(nS)} = M_{\omega(nS)}$ , see Fig. 3. Coefficients  $c_i(S = 1, L = 0, J = 1; n)$  for  $n \leq 4$  (recall that  $n$  is

radial excitation number) read:

	$\rho(1S), \omega(1S)$	$\rho(2S), \omega(2S)$	$\rho(3S), \omega(3S)$	$\rho(4S), \omega(4S)$
$i$	$\psi_1^{(1,0,1)}$	$\psi_2^{(1,0,1)}$	$\psi_3^{(1,0,1)}$	$\psi_4^{(1,0,1)}$
1	44.2	-47.0	34.4	256.1
2	147.9	96.4	367.3	-3816.4
3	-2576.7	1694.4	-6627.1	21285.8
4	10145.9	-8835.1	31300.6	-61891.6
5	-20331.5	18954.3	-72495.7	106967.9
6	23805.7	-21715.0	95497.7	-115547.6
7	-16569.8	13585.9	-73882.6	77608.2
8	6338.4	-3952.2	31633.5	-29980.2
9	-941.1	119.3	-5588.5	4927.5
10	-59.0	26.4	-333.1	258.1
11	-16.0	88.7	43.2	-25.9

(9)

For  $\rho$  and  $\omega$  mesons with dominant  $L = 2$  we have the following  $c_i(S = 1, L = 2, J = 1; n)$ :

	$\rho(1D), \omega(1D)$	$\rho(2D), \omega(2D)$	$\rho(3D), \omega(3D)$	$\rho(4D), \omega(4D)$
$i$	$\psi_1^{(1,2,1)}$	$\psi_2^{(1,2,1)}$	$\psi_3^{(1,2,1)}$	$\psi_4^{(1,2,1)}$
1	32.6	1.9	295.8	1109.3
2	-297.9	-20.8	-2587.2	-9686.9
3	1030.3	85.0	8635.8	32404.0
4	-1720.3	-207.3	-13721.7	-52043.5
5	1257.2	242.8	9530.7	36934.5
6	68.1	4.0	206.3	1219.6
7	-702.1	-203.4	-4305.9	-18749.1
8	419.2	125.4	2314.3	10789.0
9	-113.3	-25.0	-521.0	-2650.0
10	68.2	16.0	378.0	1715.0
11	-58.4	-16.6	-340.7	-1533.5

(10)

1.2.2. *Pion wave function* For the  $\pi(140)$ -meson wave function  $\psi_1^{(0,0,0)}$ , the solution obtained by spectral integral equation is rather satisfactory, it is given by the coefficients  $c_i(S = 0, L = 0, J = 0; n)$  which can be found in [6].

Still, the pion can be more precisely described by the wave function found phenomenologically, using the pion form factor data [37]. The phenomenological wave function and its parameters are as follows:

$$\psi_\pi(s) = c_\pi \left( \exp(-b_{1\pi}s) + \beta \exp(-b_{2\pi}s) \right),$$

$$c_\pi = 209.36 \text{GeV}^{-2}, \quad b_{1\pi} = 3.57 \text{GeV}^{-2}, \quad b_{2\pi} = 0.4 \text{GeV}^{-2}, \quad \beta = 0.01381. \quad (11)$$

It should be noted that the difference between the wave function of Eq. (11) and that



found in [6] is observed either at rather small relative momenta ( $k^2 = (s/4 - m^2) < 0.1$  GeV<sup>2</sup>) and or at very large ones.

*1.2.3. Pion emission constant* The pion–quark coupling  $g_\pi$  for the pion emission  $q \rightarrow \pi + q$  (diagrams of Fig. 2 type) is given by the quark form factor  $g_{\pi(140) \rightarrow q\bar{q}}(s)$  at  $s = M_\pi^2$ , namely,  $g_\pi = g_{\pi(140) \rightarrow q\bar{q}}(s = M_\pi^2)$ . However, the spectral integral equation does not determine the vertices at  $s \leq 4m^2$ , so in our present fit  $g_\pi$  is a free parameter.

Describing the widths of  $\rho(770) \rightarrow \gamma\pi(140)$  and  $\omega(780) \rightarrow \gamma\pi(140)$  with the use of vector meson (10) and pion wave functions (11), we have found two values for the pion bremsstrahlung coupling:

$$\text{Solution I : } |g_\pi| = 16.7 \pm 0.3 \begin{smallmatrix} +0.1 \\ -2.3 \end{smallmatrix}, \quad (12)$$

$$\text{Solution II : } |g_\pi| = 3.0 \pm 0.3 \begin{smallmatrix} +0.1 \\ -2.1 \end{smallmatrix}.$$

The pion emission coupling, as is well known, was a subject of investigation in physics of low-energy pion–nucleon interactions and as well as in nuclear physics. For the pion–nucleon coupling, which is determined as  $g_{\pi NN} \left( \bar{\psi}'_N(\vec{\tau}\vec{\varphi}_\pi) i\gamma_5 \psi_N \right)$ , the estimations give  $g_{\pi NN}^2/(4\pi) \simeq 14$  (see, for example, [39, 40, 41] and references therein).

We can turn the description of pion–nucleon vertex into the quark language using quark model for nucleons:

$$g_{\pi NN} \left( \bar{\psi}'_N(\vec{\tau}\vec{\varphi}_\pi) i\gamma_5 \psi_N \right) \longrightarrow g_{\pi qq} \left( \bar{\psi}'_q(\vec{\tau}\vec{\varphi}_\pi) i\gamma_5 \psi_q \right), \quad (13)$$

see Appendix A for more detail. In Eq. (12), we determine the vertex  $u \rightarrow \gamma\pi$  which is a part of the quark-language Lagrangian:

$$\begin{aligned} g_{\pi qq} \left( \bar{\psi}'_q(\vec{\tau}\vec{\varphi}_\pi) i\gamma_5 \psi_q \right) &\rightarrow \sqrt{2} g_{\pi qq} \varphi_{\pi^+}^+ \left( \bar{\psi}'_d i\gamma_5 \psi_u \right) = g_\pi \varphi_{\pi^+}^+ \left( \bar{\psi}'_d i\gamma_5 \psi_u \right), \\ \sqrt{2} g_{\pi qq} &= g_\pi. \end{aligned} \quad (14)$$

In Appendix A, we show that, making use of the SU(6)-symmetry for nucleons, one has  $g_{\pi NN} = (5/3)g_{\pi qq}$ . So, the SU(6)-symmetry provides us with  $g_{\pi NN} = (5/3\sqrt{2})g_\pi$ . It means that Solution I does not contradict the value  $g_{\pi NN}^2/(4\pi) \simeq 14$  [39, 40, 41], thus giving us

$$16.4 \leq g_{\pi NN}^2/(4\pi) \leq 23.2.$$

Note that in (12) we have included systematical errors which are due to uncertainties in the reconstruction of wave functions in the fit [6].

## 2. Gamma–pion decays of vector states $V \rightarrow \gamma\pi$

Here we present formulae which are used below for  $\rho \rightarrow \gamma\pi$  and  $\omega \rightarrow \gamma\pi$  decays.

### 2.1. Polarisation vectors, amplitude and partial width for decays

$V \rightarrow \gamma\pi$

Let us introduce notations for the momenta and polarisation vectors and define the amplitudes and decay partial widths.

2.1.1. *Polarisation vectors of the massive vector particle  $V$  and photon* Polarisations of the vector meson,  $\epsilon_\mu^{(V)}$ , and of virtual photon,  $\epsilon_\alpha^{(\gamma^*)}$ , are the transverse vectors:

$$\epsilon_\beta^{(V)} p_\beta = 0, \quad \epsilon_\alpha^{(\gamma^*)} q_\alpha = 0, \quad (15)$$

where  $q$  is the virtual photon four-momentum ( $q^2 \neq 0$ ) and  $p$  is that of the vector meson ( $p^2 = M_V^2$ ). Polarisation of the vector meson obeys the completeness condition as follows:

$$-\sum_{a=1,2,3} \epsilon_\mu^{(V)}(a) \epsilon_{\mu'}^{(V)+}(a) = g_{\mu\mu'}^{\perp V} \equiv g_{\mu\mu'}^{\perp p}, \quad g_{\mu\mu'}^{\perp p} = g_{\mu\mu'} - \frac{p_\mu p_{\mu'}}{p^2}, \quad (16)$$

where  $g_{\mu\mu'}^{\perp p}$  is the metric tensor operating in the space orthogonal to the momentum  $p$ .

For virtual photon, ( $q^2 \neq 0$ ), the completeness condition for polarisation vectors is written in three-dimensional space:

$$-\sum_{a=1,2,3} \epsilon_\alpha^{(\gamma^*)}(a) \epsilon_{\alpha'}^{(\gamma^*)+}(a) = g_{\alpha\alpha'}^{\perp \gamma^*}, \quad g_{\alpha\alpha'}^{\perp \gamma^*} \equiv g_{\alpha\alpha'}^{\perp q} = g_{\alpha\alpha'} - \frac{q_\alpha q_{\alpha'}}{q^2}. \quad (17)$$

The polarisation vector of the real photon ( $q^2 = 0$ ) denoted as  $\epsilon_\alpha^\gamma$  has two independent components only, they are orthogonal to the reaction plane:

$$\epsilon_\alpha^{(\gamma)} q_\alpha = 0, \quad \epsilon_\alpha^{(\gamma)} p_\alpha = 0. \quad (18)$$

Likewise, the completeness condition for the real photon reads:

$$-\sum_{a=1,2} \epsilon_\alpha^{(\gamma)}(a) \epsilon_{\alpha'}^{(\gamma)+}(a) = g_{\alpha\alpha'}^{\perp\perp}, \quad (19)$$

$$g_{\alpha\alpha'}^{\perp\perp} = g_{\alpha\alpha'} - \frac{p_\alpha p_{\alpha'}}{p^2} - \frac{q_\alpha^\perp q_{\alpha'}^\perp}{q_\perp^2}, \quad q_\alpha^\perp \equiv g_{\alpha\alpha'}^{\perp V} q_{\alpha'} = q_\alpha - \frac{(pq)}{p^2} p_\alpha.$$

2.1.2. *Amplitude for the decay  $V \rightarrow \gamma\pi$*  The decay amplitude  $V \rightarrow \gamma\pi$  is written as a product of the spin structure and form factor:

$$A_{V \rightarrow \gamma\pi} = \epsilon_\alpha^{(\gamma)} \epsilon_\mu^{(V)} A_{\alpha\mu}^{(V \rightarrow \gamma\pi)},$$

$$A_{\alpha\mu}^{(V \rightarrow \gamma\pi)} = e S_{\alpha\mu}^{(V \rightarrow \gamma\pi)}(p, q) F^{V \rightarrow \gamma\pi}(0, M_\pi^2), \quad (20)$$

with

$$S_{\alpha\mu}^{(V \rightarrow \gamma\pi)}(p, q) = \varepsilon_{\alpha\mu pq} \equiv \varepsilon_{\alpha\mu\nu_1\nu_2} p_{\nu_1} q_{\nu_2}. \quad (21)$$

In (20), the electron charge  $e$  is singled out, and in (21) the tensor  $\varepsilon_{\alpha\mu\nu_1\nu_2}$  is the wholly antisymmetrical. Let us emphasise the specific role of the spin operator  $\varepsilon_{\alpha\mu pq}$ . Since  $\varepsilon_{\alpha\mu pp} = 0$ , this spin operator is valid for the reaction with both real ( $\gamma$ ) and virtual ( $\gamma^*$ ) photons, so Eq. (20) can be used for the transition with virtual photon, with corresponding substitution:  $F^{V \rightarrow \gamma\pi}(0) \rightarrow F^{V \rightarrow \gamma\pi}(q^2)$ .

2.1.3. *Partial width for  $V \rightarrow \gamma\pi$*  The partial width for the decay  $V \rightarrow \gamma\pi$  is determined as follows:

$$M_V \Gamma_{V \rightarrow \gamma\pi} = \frac{1}{3} \int d\Phi_2(p; q, p_\pi) \left| \sum_{\alpha\mu} A_{\alpha\mu}^{(V \rightarrow \gamma\pi)} \right|^2 =$$

$$\begin{aligned}
&= \frac{\alpha}{24} \frac{(M_V^2 - M_\pi^2)^3}{M_V^2} |F^{V \rightarrow \gamma\pi}(0, M_\pi^2)|^2, \\
d\Phi_2(p; q, p_\pi) &= \frac{1}{2} \frac{d^3q}{(2\pi)^3} \frac{d^3p_\pi}{2q_0 (2\pi)^3 2p_{\pi 0}} (2\pi)^4 \delta^{(4)}(p - q - p_\pi). \quad (22)
\end{aligned}$$

The summation is carried out over the photon and vector meson polarisation  $s$ , and  $(\varepsilon_{\alpha\mu\rho q})^2 = (M_V^2 - M_\pi^2)^2/2$ . In the final expression  $\alpha = e^2/4\pi = 1/137$ .

## 2.2. Double spectral integral representation of the triangle diagrams with photon emission

To derive double spectral integral for the form factors with photon emission by quark and antiquark,  $F_{\Delta\gamma}^{V(L) \rightarrow \gamma\pi}(q^2)$  and  $F_{\nabla\gamma}^{V(L) \rightarrow \gamma\pi}(q^2)$ , see Fig. 1, one needs to calculate the double discontinuities of the triangle diagrams.

*2.2.1. Double discontinuities of the triangle diagrams* First, consider the photon emission by quark, see Fig. 1a. Corresponding cuttings for the calculation of double discontinuity are shown in Fig. 1b.

In the dispersion representation, the invariant energy in the intermediate state differs from that in the initial and final states. Because of that, at the double discontinuity  $P \neq p$  and  $P' \neq p_\pi$ . The following requirements are imposed on the momenta shown in the diagram of Fig. 1b [23, 38]:

$$(k_1 + k_2)^2 = P^2 \equiv s > 4m^2, \quad (k'_1 + k_2)^2 = P'^2 \equiv s' > 4m^2. \quad (23)$$

The momentum squared of the photon,  $q^2$ , is fixed:

$$(p - p_\pi)^2 = (P - P')^2 = (k_1 - k'_1)^2 = q^2. \quad (24)$$

When cutting Feynman diagram, the propagators should be substituted by the residues in the poles. This is equivalent to the replacement as follows:  $(m^2 - k_1^2)^{-1} \rightarrow \delta(m^2 - k_1^2)$ ,  $(m^2 - k_2^2)^{-1} \rightarrow \delta(m^2 - k_2^2)$  and  $(m^2 - k_1'^2)^{-1} \rightarrow \delta(m^2 - k_1'^2)$ , so the intermediate-state quarks are mass-on-shell:

$$k_1^2 = k_2^2 = k_1'^2 = m^2. \quad (25)$$

Then, for the diagram with photon emitted by quark (Fig. 1a), the double discontinuity of the amplitude (Fig. 1b) becomes proportional to the three factors:

$$\begin{aligned}
&\text{disc}_s \text{disc}_{s'} A_{\alpha\mu}^{V(L) \rightarrow \gamma\pi}(\Delta\gamma) \sim Z_{\Delta\gamma}^{V \rightarrow \gamma\pi} G_{V(L)}(s) G_\pi(s') \\
&\times d\Phi_2(P; k_1, k_2) d\Phi_2(P'; k'_1, k'_2) (2\pi)^3 2k_{20} \delta^3(\vec{k}'_2 - \vec{k}_2) \\
&\times \text{Sp} \left[ Q_\mu^{V(L)}(k) (\hat{k}_1 + m) Q_\alpha^{(\gamma)}(\hat{k}'_1 + m) Q^{(\pi)}(-\hat{k}_2 + m) \right]. \quad (26)
\end{aligned}$$

The first factor in the right-hand side of (26) consists of the following vertices: the quark charge factor  $Z_{\Delta\gamma}^{V \rightarrow \gamma\pi}$  as well as transition vertices  $V(L) \rightarrow q\bar{q}$  and  $\pi \rightarrow q\bar{q}$  which are denoted as  $G_{V(L)}(s)$  and  $G_\pi(s')$ .

The second factor contains space volumes of the two-particle states,  $d\Phi_2(P; k_1, k_2)$  and  $d\Phi_2(P'; k'_1, k'_2)$ , which correspond to two cuts shown in the diagram of Fig. 1b (the

space volume is determined in (22)). The factor  $(2\pi)^3 2k_{20} \delta^3(\vec{k}'_2 - \vec{k}_2)$  takes into account the fact that one quark line is cut twice.

The third factor in (26) is the trace coming from the summation over the quark spin states. Since the spin factor in the transition  $V \rightarrow q\bar{q}$  may be of two types (with dominant  $S$ - or dominant  $D$ -wave), we have the following operators for virtual photon,  $Q_\mu^{V(L)}$ , see Eq. (6):

$$\begin{aligned} Q_\mu^{V(L=0)}(k) &= \gamma_\mu^{\perp V} = \gamma_\mu^{\perp P} \equiv g_{\mu\mu'}^{\perp P} \gamma_{\mu'}, \\ Q_\mu^{V(L=2)}(k) &= \sqrt{2} \gamma_{\mu'} X_{\mu'\mu}^{(2)}(k) = \frac{3}{\sqrt{2}} \left[ k_\mu \hat{k} - \frac{1}{3} k^2 \gamma_\mu^{\perp P} \right], \end{aligned} \quad (27)$$

and for the pion:

$$Q^{(\pi)} = i\gamma_5. \quad (28)$$

Here,  $k = (k_1 - k_2)/2$  is the relative momentum of the incoming quarks,  $k \perp P = k_1 + k_2$ , i.e.  $k = k_1^{\perp P} = -k_2^{\perp P}$ .

For real photon, we replace:

$$\begin{aligned} Q_\alpha^{(\gamma)} &\rightarrow Q_\alpha^{\perp\perp} \equiv \gamma_\alpha^{\perp\perp}(P, P') = g_{\alpha\alpha'}^{\perp\perp}(P, P') \gamma_{\alpha'}, \\ g_{\alpha\alpha'}^{\perp\perp}(P, P') P_{\alpha'} &= 0, \quad g_{\alpha\alpha'}^{\perp\perp}(P, P') P'_{\alpha'} = 0, \end{aligned} \quad (29)$$

where  $(P - P')^2 = 0$ . The metric tensor  $g_{\alpha\alpha'}^{\perp\perp}(P, P')$  works in the space orthogonal to the intermediate state momenta:  $g_{\alpha\alpha'}^{\perp\perp}(P, P') = g_{\alpha\alpha'} - P_\alpha P_{\alpha'} / P^2 - P'_\alpha{}^{\perp P} P'_{\alpha'}{}^{\perp P} / P_\alpha{}^{\perp P} P_{\alpha'}{}^{\perp P}$ .

Actually, for the real photon we can use simpler operator, say,  $Q_\alpha^{(\gamma)} = \gamma_\alpha^\perp$ , because in the considered decay we should have the same result for both choices,  $Q_\alpha^{(\gamma)}$  or  $Q_\alpha^{\perp\perp}$ , due to the spin operator structure (21). However, here we use (29) to emphasise an important point for this type of reactions: the amplitude for transversely polarized photons is determined by the spectral integral with transversely polarized photons in the intermediate states as well.

For the photon emission, there are two diagrams: the second one is similar to that of Fig. 1a but with the emission of photon by antiquark, it is shown in Fig. 1c. The double discontinuity of the corresponding amplitude is determined by cuttings shown in Fig. 1d:

$$\begin{aligned} \text{disc}_s \text{disc}_{s'} A_{\alpha\mu}^{V(L) \rightarrow \gamma\pi}(\nabla_\gamma) &\sim Z_{V \rightarrow \gamma\pi}(\nabla_\gamma) G_{V(L)}(s) G_\pi(s') \\ &\times d\Phi_2(P; k_1, k_2) d\Phi_2(P'; k'_1, k'_2) (2\pi)^3 2k_{10} \delta^3(\vec{k}'_1 - \vec{k}_1) \\ &\times \text{Sp} \left[ Q_\mu^{V(L)}(k) (\hat{k}_1 + m) Q^{(\pi)}(-\hat{k}'_2 + m) Q_\alpha^{(\gamma)}(-\hat{k}_2 + m) \right]. \end{aligned} \quad (30)$$

Likewise, there are two traces for two transitions with photon emission by quark and antiquark:

$$\begin{aligned} S p_{\alpha\mu}^{V(L) \rightarrow \gamma\pi}(\Delta_\gamma) &= -\text{Sp} \left[ Q_\mu^{V(L)}(k) (\hat{k}_1 + m) Q_\alpha^{(\gamma)}(\hat{k}'_1 + m) Q^{(\pi)}(-\hat{k}_2 + m) \right], \\ S p_{\alpha\mu}^{V(L) \rightarrow \gamma\pi}(\nabla_\gamma) &= -\text{Sp} \left[ Q_\mu^{V(L)}(k) (\hat{k}_1 + m) Q^{(\pi)}(-\hat{k}'_2 + m) Q_\alpha^{(\gamma)}(-\hat{k}_2 + m) \right]. \end{aligned} \quad (31)$$

To calculate the invariant form factors  $F_{\Delta\gamma}^{V(L)\rightarrow\gamma\pi}(0)$  and  $F_{\nabla\gamma}^{V(L)\rightarrow\gamma\pi}(0)$ , we should extract from (31) the intermediate-state spin operator:

$$S_{\alpha\mu}^{(V\rightarrow\gamma\pi)}(P, \tilde{q}) = \varepsilon_{\alpha\mu P\tilde{q}}, \quad \tilde{q} = P - P'. \quad (32)$$

Therefore, we have:

$$\begin{aligned} Sp_{\alpha\mu}^{V(L)\rightarrow\gamma\pi}(\Delta\gamma) &= S_{\alpha\mu}^{(V\rightarrow\gamma\pi)}(P, \tilde{q})S_{\Delta\gamma}^{V(L)\rightarrow\gamma\pi}(s, s', q^2), \\ Sp_{\alpha\mu}^{V(L)\rightarrow\gamma\pi}(\nabla\gamma) &= S_{\alpha\mu}^{(V\rightarrow\gamma\pi)}(P, \tilde{q})S_{\nabla\gamma}^{V(L)\rightarrow\gamma\pi}(s, s', q^2), \end{aligned} \quad (33)$$

where

$$\begin{aligned} \frac{(Sp_{\alpha\mu}^{V(L)\rightarrow\gamma\pi}(\Delta\gamma)S_{\alpha\mu}^{(V\rightarrow\gamma\pi)}(P, \tilde{q}))}{(S_{\alpha\mu}^{(V\rightarrow\gamma\pi)}(P, \tilde{q}))^2} &= S_{\Delta\gamma}^{V(L)\rightarrow\gamma\pi}(s, s', q^2), \\ \frac{(Sp_{\alpha\mu}^{V(L)\rightarrow\gamma\pi}(\nabla\gamma)S_{\alpha\mu}^{(V\rightarrow\gamma\pi)}(P, \tilde{q}))}{(S_{\alpha\mu}^{(V\rightarrow\gamma\pi)}(P, \tilde{q}))^2} &= S_{\nabla\gamma}^{V(L)\rightarrow\gamma\pi}(s, s', q^2). \end{aligned} \quad (34)$$

Taking into account the expression  $\text{Sp}[\gamma_5\gamma_{\alpha_1}\gamma_{\alpha_2}\gamma_{\alpha_3}\gamma_{\alpha_4}] = 4i\varepsilon_{\alpha_1\alpha_2\alpha_3\alpha_4}$  we obtain:

$$\begin{aligned} S_{\Delta\gamma}^{V(L=0)\rightarrow\gamma\pi}(s, s', q^2) &= S_{\nabla\gamma}^{V(0)\rightarrow\gamma\pi}(s, s', q^2) = -4m, \\ S_{\Delta\gamma}^{V(L=2)\rightarrow\gamma\pi}(s, s', q^2) &= S_{\nabla\gamma}^{V(2)\rightarrow\gamma\pi}(s, s', q^2) = -\frac{m}{\sqrt{2}} \left[ 2m^2 + s + \frac{6ss'q^2}{\lambda(s, s', q^2)} \right], \end{aligned} \quad (35)$$

with

$$\lambda(s, s', q^2) = (s - s')^2 - 2q^2(s + s') + q^4. \quad (36)$$

The photon emission amplitude, being determined by two diagrams of Fig. 1a and Fig. 1c, reads

$$A_{(\Delta\gamma+\nabla\gamma)\alpha\mu}^{V(L)\rightarrow\gamma\pi} = e\varepsilon_{\alpha\mu pq} \left[ Z_{\Delta\gamma}^{V\rightarrow\gamma\pi} F_{\Delta\gamma}^{V(L)\rightarrow\gamma\pi}(q^2, M_\pi^2) + Z_{\nabla\gamma}^{V\rightarrow\gamma\pi} F_{\nabla\gamma}^{V(L)\rightarrow\gamma\pi}(q^2, M_\pi^2) \right], \quad (37)$$

while the double discontinuities of the form factors in (37) are equal to:

$$\begin{aligned} \text{disc}_s \text{disc}_{s'} F_{\Delta\gamma}^{V(L)\rightarrow\gamma\pi}(q^2, M_\pi^2) &= G_{V(L)}(s)G_\pi(s') \\ &\times d\Phi_2(P; k_1, k_2)d\Phi_2(P'; k'_1, k'_2)(2\pi)^3 2k_{20}\delta^3(\vec{k}'_2 - \vec{k}_2)S_{\Delta\gamma}^{V(L)\rightarrow\gamma\pi}(s, s', q^2), \\ \text{disc}_s \text{disc}_{s'} F_{\nabla\gamma}^{V(L)\rightarrow\gamma\pi}(q^2, M_\pi^2) &= G_{V(L)}(s)G_\pi(s') \\ &\times d\Phi_2(P; k_1, k_2)d\Phi_2(P'; k'_1, k'_2)(2\pi)^3 2k_{10}\delta^3(\vec{k}'_1 - \vec{k}_1)S_{\nabla\gamma}^{V(L)\rightarrow\gamma\pi}(s, s', q^2). \end{aligned} \quad (38)$$

*2.2.2. The double spectral integral for the form factors with photon emission by quark and antiquark* The equation (38) defines the form factor through the dispersion integral as follows:

$$\begin{aligned} F_{\Delta\gamma}^{V(L)\rightarrow\gamma\pi}(q^2, M_\pi^2) &= \int_{4m^2}^{\infty} \frac{ds}{\pi} \int_{4m^2}^{\infty} \frac{ds'}{\pi} \frac{\text{disc}_s \text{disc}_{s'} F_{\Delta\gamma}^{V(L)\rightarrow\gamma\pi}(q^2, M_\pi^2)}{(s - M_{V(L)}^2)(s' - M_\pi^2)}, \\ F_{\nabla\gamma}^{V(L)\rightarrow\gamma\pi}(q^2, M_\pi^2) &= \int_{4m^2}^{\infty} \frac{ds}{\pi} \int_{4m^2}^{\infty} \frac{ds'}{\pi} \frac{\text{disc}_s \text{disc}_{s'} F_{\nabla\gamma}^{V(L)\rightarrow\gamma\pi}(q^2, M_\pi^2)}{(s - M_{V(L)}^2)(s' - M_\pi^2)}. \end{aligned} \quad (39)$$

We have

$$F_{\Delta\gamma}^{V(L)\rightarrow\gamma\pi}(q^2, M_\pi^2) = F_{\nabla\gamma}^{V(L)\rightarrow\gamma\pi}(q^2, M_\pi^2) \quad (40)$$

at equal masses of the quark and antiquark – just this case is considered here. In (39), we omit subtraction terms, assuming that the convergence of (39) is guaranteed by the vertices  $G_{V(L)}(s)$  and  $G_\pi(s')$ . Furthermore, we define the wave functions of the  $q\bar{q}$  systems:  $\psi_{V(L)}(s) = G_{V(L)}(s)/(s - M_{V(L)}^2)$  and  $\psi_\pi(s') = G_\pi(s')/(s' - M_\pi^2)$ .

After integrating over the momenta in accordance with (38), one can represent (39) in the following form:

$$F_{\Delta\gamma}^{V(L)\rightarrow\gamma\pi}(q^2, M_\pi^2) = F_{\nabla\gamma}^{V(L)\rightarrow\gamma\pi}(q^2, M_\pi^2) = \int_{4m^2}^{\infty} \frac{ds ds'}{16\pi^2} \psi_{V(L)}(s) \psi_\pi(s') \times \frac{\Theta(-ss'q^2 - m^2\lambda(s, s', q^2))}{\sqrt{\lambda(s, s', q^2)}} S_{\Delta\gamma}^{V(L)\rightarrow\gamma\pi}(s, s', q^2), \quad (41)$$

where  $\Theta(X)$  is the step-function:  $\Theta(X) = 1$  at  $X \geq 0$  and  $\Theta(X) = 0$  at  $X < 0$ .

**2.2.3. Z-factors for photon emission** For the  $\rho^+$  meson, the photon emission is determined by two diagrams, see Figs. 4a and 4b, which give us the following charge factors:

$$Z_{\Delta\gamma}^{\rho^+\rightarrow\gamma\pi^+} = e_u = \frac{2}{3}, \quad Z_{\nabla\gamma}^{\rho^+\rightarrow\gamma\pi^+} = e_d = -\frac{1}{3}. \quad (42)$$

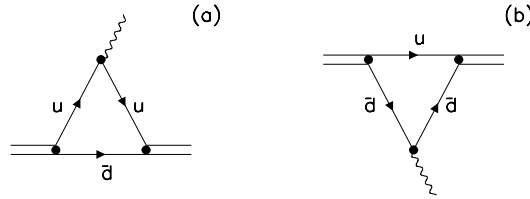


**Figure 4.** Diagrams for the determination of Z-factors in the reaction  $\rho^+ \rightarrow \gamma\pi^+$  with photon emission .

For neutral vector mesons ( $\rho^0$ ,  $\omega$ ), we have four diagrams, see Fig. 5, which result in the charge factors as follows:

$$Z_{\Delta\gamma}^{\rho^0\rightarrow\gamma\pi^0} = Z_{\nabla\gamma}^{\rho^0\rightarrow\gamma\pi^0} = \frac{1}{2}(e_u + e_d) = \frac{1}{6},$$

$$Z_{\Delta\gamma}^{\omega\rightarrow\gamma\pi^0} = Z_{\nabla\gamma}^{\omega\rightarrow\gamma\pi^0} = \frac{1}{2}(e_u - e_d) = \frac{1}{2}. \quad (43)$$

In (43), we use the standard flavour wave functions for ( $I = 1, I_3 = 0$ ) and ( $I = 0, I_3 = 0$ ) states:  $\rho^0 = \pi^0 = (u\bar{u} - d\bar{d})/\sqrt{2}$  and  $\omega = (u\bar{u} + d\bar{d})/\sqrt{2}$ .

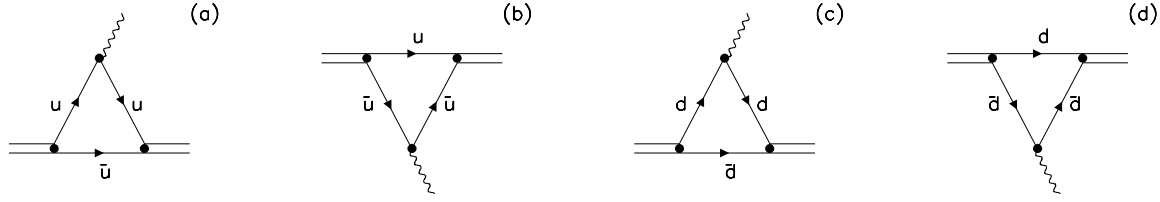


**Figure 5.** Diagrams for the determination of Z-factors in the reactions  $\rho^0 \rightarrow \gamma\pi^0$  and  $\omega^0 \rightarrow \gamma\pi^0$  with photon emission.

2.2.4. *Decay form factors at  $Q^2 = -q^2 \rightarrow 0$*  To calculate the integral at small  $Q^2$ , we substitute:

$$s = \Sigma + \frac{1}{2}zQ, \quad s' = \Sigma - \frac{1}{2}zQ, \quad q^2 = -Q^2. \quad (44)$$

In the region  $Q^2 \ll 4m^2$ , the form factors (41) can be written as

$$\begin{aligned} F_{\Delta\gamma}^{V(L)\rightarrow\gamma\pi}(-Q^2, M_\pi^2) &= F_{\nabla\gamma}^{V(L)\rightarrow\gamma\pi}(-Q^2, M_\pi^2) = \int_{4m^2}^{\infty} \frac{d\Sigma}{\pi} \psi_{V(L)}(\Sigma) \psi_\pi(\Sigma) \\ &\times \int_{-b}^{+b} \frac{dz}{\pi} \frac{S_{\Delta\gamma}^{V(L)\rightarrow\gamma\pi}(\Sigma + \frac{1}{2}zQ, \Sigma - \frac{1}{2}zQ, -Q^2)}{16\sqrt{\Lambda(\Sigma, z, Q^2)}}, \\ b &= \sqrt{\Sigma\left(\frac{\Sigma}{m^2} - 4\right)}, \quad \Lambda(\Sigma, z, Q^2) = (z^2 + 4\Sigma)Q^2. \end{aligned} \quad (45)$$

After integrating over  $z$  and substituting  $\Sigma \rightarrow s$ , the form factors for  $L = 0, 2$  read:

$$\begin{aligned} F_{\Delta\gamma}^{V(0)\rightarrow\gamma\pi}(0, M_\pi^2) &= F_{\nabla\gamma}^{V(0)\rightarrow\gamma\pi}(0, M_\pi^2) = -4m \int_{4m^2}^{\infty} \frac{ds}{16\pi^2} \psi_\pi(s) \psi_{V(0)}(s) \\ &\times \ln \frac{s + \sqrt{s(s - 4m^2)}}{s - \sqrt{s(s - 4m^2)}}, \\ F_{\Delta\gamma}^{V(2)\rightarrow\gamma\pi}(0, M_\pi^2) &= F_{\nabla\gamma}^{V(2)\rightarrow\gamma\pi}(0, M_\pi^2) = -m/\sqrt{2} \int_{4m^2}^{\infty} \frac{ds}{4\pi^2} \psi_\pi(s) \psi_{V(2)}(s) \\ &\times \left[ (2m^2 + s) \ln \frac{\sqrt{s} + \sqrt{s - 4m^2}}{\sqrt{s} - \sqrt{s - 4m^2}} + 3\sqrt{s(s - 4m^2)} \right]. \end{aligned} \quad (46)$$

Remind that wave functions  $\psi_{V(0)}(s) = \psi_n^{(1,0,1)}(k^2)$ ,  $\psi_{V(2)}(s) = \psi_n^{(1,2,1)}(k^2)$  and  $\psi_\pi(s)$  are presented in Section I.

2.2.5. *Normalisation conditions for the wave functions  $\psi_\pi(s)$  and  $\psi_{V(L=0,2)}(s)$*  It is convenient to write the normalisation conditions for  $\psi_\pi(s)$  and  $\psi_{V(L)}(s)$  using the charge form factor of a meson:

$$F_{charge}(0) = 1. \quad (47)$$

The amplitude of the charge factor is defined by the photon-emission triangle diagram with  $(q\bar{q})_{in} = (q\bar{q})_{out}$ . For the pion, the amplitude takes the form:

$$A_\alpha(q) = e(p + p_\pi)_\alpha F_{charge}(q^2), \quad (48)$$

while  $F_{charge}(q^2)$  can be calculated in the same way as the transition form factors considered above. The normalisation condition for pion reads:

$$1 = \int_{4m^2}^{\infty} \frac{ds}{16\pi^2} \psi_\pi^2(s) 2s \sqrt{\frac{s-4m^2}{s}}. \quad (49)$$

For vector meson  $V(L)$ , the normalisation condition may be determined by averaging over spins of the massive vector particle, see [2, 3, 42, 43] for detail. Then, the normalisation condition reads:

$$\begin{aligned} 1 &= \frac{1}{3} \int_{4m^2}^{\infty} \frac{ds}{16\pi^2} \psi_{V(0)}^2(s) 4(s+2m^2) \sqrt{\frac{s-4m^2}{s}}, \\ 1 &= \frac{1}{3} \int_{4m^2}^{\infty} \frac{ds}{16\pi^2} \psi_{V(2)}^2(s) \frac{(8m^2+s)(s-4m^2)^2}{8} \sqrt{\frac{s-4m^2}{s}}. \end{aligned} \quad (50)$$

Recall that here  $\psi_{V(0)}(s) = \psi_n^{(1,0,1)}(k^2)$  and  $\psi_{V(2)}(s) = \psi_n^{(1,2,1)}(k^2)$  with  $k^2 = s/4 - m^2$ .

### 2.2.6. Vector mesons: normalisation condition in case of two-component wave functions

In the solution found in [6], the wave functions  $\psi_{V(0)}$  and  $\psi_{V(2)}$  are orthogonal to each other with a good accuracy. Generally, vector states may mix. Then the vector mesons have two-component wave functions, see (7), and normalisation condition reads:

$$\begin{aligned} \delta_{ab} &= \frac{1}{3} \int_{4m^2}^{\infty} \frac{ds}{16\pi^2} C_{a0}^{(n)} C_{b0}^{(n)} \left( \psi_n^{(1,0,1)}(k^2) \right)^2 4(s+2m^2) \sqrt{\frac{s-4m^2}{s}} \\ &+ \frac{1}{3} \int_{4m^2}^{\infty} \frac{ds}{16\pi^2} \left( C_{a0}^{(n)} C_{b2}^{(n)} + C_{b0}^{(n)} C_{a2}^{(n)} \right) \psi_n^{(1,0,1)}(k^2) \psi_n^{(1,2,1)}(k^2) \\ &\quad \times \sqrt{2} \frac{(s-4m^2)^2}{6} \sqrt{\frac{s-4m^2}{s}} \\ &+ \frac{1}{3} \int_{4m^2}^{\infty} \frac{ds}{16\pi^2} C_{a2}^{(n)} C_{b2}^{(n)} \left( \psi_n^{(1,2,1)}(k^2) \right)^2 \\ &\quad \times \frac{(8m^2+s)(s-4m^2)^2}{8} \sqrt{\frac{s-4m^2}{s}}. \end{aligned} \quad (51)$$

## 3. Double spectral integral representation of the triangle diagrams with pion emission

Here, we calculate the double spectral integral for the transition form factors with the emission of pion by quark,  $F_{\Delta_\pi}^{V(L) \rightarrow \gamma\pi}(0, M_\pi^2)$  (diagram of Fig. 2a) and antiquark,  $F_{\nabla_\pi}^{V(L) \rightarrow \gamma\pi}(0, M_\pi^2)$  (diagram of Fig. 2c).



3.0.7. *Double discontinuities of the triangle diagrams* For the diagram of Fig. 2a, the cuttings are shown in Fig. 2b, with the following notations:

$$\begin{aligned} k_1^2 &= k_2^2 = k_1'^2 = m^2, \\ (k_1 + k_2)^2 &= P^2 \equiv s > 4m^2, \quad (k_1' + k_2)^2 = P'^2 \equiv s' > 4m^2, \\ (P - P')^2 &= (k_1 - k_1')^2 = p_\pi^2 = M_\pi^2. \end{aligned} \quad (52)$$

For the diagram of Fig. 2a, the double discontinuity, determined by Fig. 2b, contains three factors:

$$\begin{aligned} \text{disc}_s \text{disc}_{s'} A_{\alpha\mu}^{V(L) \rightarrow \gamma\pi}(\Delta^\pi) &\sim Z_{V \rightarrow \gamma\pi}(\Delta^\pi) g_\pi G_{V(L)}(s) G_\gamma(s') \\ &\times d\Phi_2(P; k_1, k_2) d\Phi_2(P'; k_1', k_2') (2\pi)^3 2k_{20} \delta^3(\vec{k}_2' - \vec{k}_2) \\ &\times \text{Sp} \left[ Q_\mu^{V(L)}(k) (\hat{k}_1 + m) Q^{(\pi)}(\hat{k}_1' + m) Q_\alpha^{(\gamma\perp)}(-\hat{k}_2 + m) \right]. \end{aligned} \quad (53)$$

The right-hand side of (53) is determined by the the quark charge factor  $Z_{V \rightarrow \gamma\pi}(\Delta^\pi)$ , the transition vertices  $V(L) \rightarrow q\bar{q}$  and  $\gamma \rightarrow q\bar{q}$  and pion–quark coupling  $g_\pi$ . The trace in (53) contains the operators  $Q^{(\pi)}$  and  $Q_\alpha^{(\gamma\perp)}$  which are determined in (29):  $Q_\alpha^{(\gamma\perp)} = \gamma_\alpha^{\perp\perp}(P, P')$  and  $Q^{(\pi)} = i\gamma_5$ .

The diagram with the emission of pion by antiquark is shown in Fig. 2c. The double discontinuity of the corresponding amplitude, Fig. 2d, is written similarly to (53). We have:

$$\begin{aligned} \text{disc}_s \text{disc}_{s'} A_{\alpha\mu}^{V(L) \rightarrow \gamma\pi}(\nabla_\pi) &\sim Z_{V \rightarrow \gamma\pi}(\nabla_\pi) g_\pi G_{V(L)}(s) G_\gamma(s') \\ &\times d\Phi_2(P; k_1, k_2) d\Phi_2(P'; k_1', k_2') (2\pi)^3 2k_{10} \delta^3(\vec{k}_1' - \vec{k}_1) \\ &\times \text{Sp} \left[ Q_\mu^{V(L)}(k) (\hat{k}_1 + m) Q_\alpha^{(\gamma\perp)}(-\hat{k}_2' + m) Q^{(\pi)}(-\hat{k}_2 + m) \right]. \end{aligned} \quad (54)$$

Correspondingly, we have two traces for two transitions with pion emission by the quark and antiquark:

$$\begin{aligned} Sp_{\alpha\mu}^{V(L) \rightarrow \gamma\pi}(\Delta^\pi) &= -\text{Sp} \left[ Q_\mu^{V(L)}(k) (\hat{k}_1 + m) Q^{(\pi)}(\hat{k}_1' + m) Q_\alpha^{(\gamma\perp)}(-\hat{k}_2 + m) \right] \\ &= S_{\alpha\mu}^{(V \rightarrow \gamma\pi)}(P, P - P') S_{\Delta^\pi}^{V(L) \rightarrow \gamma\pi}(s, s', (P - P')^2), \\ Sp_{\alpha\mu}^{V(L) \rightarrow \gamma\pi}(\nabla_\pi) &= -\text{Sp} \left[ Q_\mu^{V(L)}(k) (\hat{k}_1 + m) Q_\alpha^{(\gamma\perp)}(-\hat{k}_2' + m) Q^{(\pi)}(-\hat{k}_2 + m) \right] \\ &= S_{\alpha\mu}^{(V \rightarrow \gamma\pi)}(P, P - P') S_{\nabla_\pi}^{V(L) \rightarrow \gamma\pi}(s, s', (P - P')^2), \\ S_{\alpha\mu}^{(V \rightarrow \gamma\pi)}(P, P - P') &= \varepsilon_{\alpha\mu P(P-P')} = -\varepsilon_{\alpha\mu P P'}. \end{aligned} \quad (55)$$

Here,

$$\begin{aligned} \frac{(Sp_{\alpha\mu}^{V(L) \rightarrow \gamma\pi}(\Delta^\pi) S_{\alpha\mu}^{(V \rightarrow \gamma\pi)}(P, P - P'))}{(S_{\alpha\mu}^{(V \rightarrow \gamma\pi)}(P, P - P'))^2} &= S_{\Delta^\pi}^{V(L) \rightarrow \gamma\pi}(s, s', (P - P')^2), \\ \frac{(Sp_{\alpha\mu}^{V(L) \rightarrow \gamma\pi}(\nabla_\pi) S_{\alpha\mu}^{(V \rightarrow \gamma\pi)}(P, P - P'))}{(S_{\alpha\mu}^{(V \rightarrow \gamma\pi)}(P, P - P'))^2} &= S_{\nabla_\pi}^{V(L) \rightarrow \gamma\pi}(s, s', (P - P')^2). \end{aligned} \quad (56)$$

As a result, we obtain:

$$S_{\Delta^\pi}^{V(0) \rightarrow \gamma\pi}(s, s', (P - P')^2) = S_{\nabla_\pi}^{V(0) \rightarrow \gamma\pi}(s, s', (P - P')^2) = 4m,$$

$$\begin{aligned} S_{\Delta\pi}^{V(2)\rightarrow\gamma\pi}(s, s', (P-P')^2) &= S_{\nabla\pi}^{V(2)\rightarrow\gamma\pi}(s, s', (P-P')^2) \\ &= \frac{m}{\sqrt{2}} \left[ 2m^2 + s + \frac{6ss'(P-P')^2}{\lambda(s, s', (P-P')^2)} \right]. \end{aligned} \quad (57)$$

Let us note that spin factors  $S_{\Delta\pi}^{V(0)\rightarrow\gamma\pi}(s, s', (P-P')^2)$  and  $S_{\Delta\pi}^{V(2)\rightarrow\gamma\pi}(s, s', (P-P')^2)$  differ by the sign only from those for photon emission  $S_{\Delta\gamma}^{V(0)\rightarrow\gamma\pi}(s, s', q^2)$  and  $S_{\Delta\gamma}^{V(2)\rightarrow\gamma\pi}(s, s', q^2)$ , given by (35). The pion emission amplitude, considered as a function of  $q^2$  and  $p_\pi^2$ , is determined by two processes (Figs. 2a, 2c):

$$\begin{aligned} A_{\alpha\mu}^{(V(L)\rightarrow\gamma\pi)}(\Delta^\pi + \nabla_\pi) &= e \varepsilon_{\alpha\mu pq} \\ &\times \left[ Z_{\Delta\pi}^{V\rightarrow\gamma\pi} F_{\Delta\pi}^{V(L)\rightarrow\gamma\pi}(q^2, p_\pi^2) + Z_{\nabla\pi}^{V\rightarrow\gamma\pi} F_{\nabla\pi}^{V(L)\rightarrow\gamma\pi}(q^2, p_\pi^2) \right], \end{aligned} \quad (58)$$

with

$$F_{\Delta\pi}^{V(L)\rightarrow\gamma\pi}(q^2, p_\pi^2) = F_{\nabla\pi}^{V(L)\rightarrow\gamma\pi}(q^2, p_\pi^2) \quad (59)$$

due to the equality (57)

$$\text{disc}_s \text{disc}_{s'} F_{\Delta\pi}^{V(L)\rightarrow\gamma\pi}(s', p_\pi^2) = \text{disc}_s \text{disc}_{s'} F_{\nabla\pi}^{V(L)\rightarrow\gamma\pi}(s', p_\pi^2). \quad (60)$$

*3.0.8. The double spectral integral for the form factors with pion emission* The form factors read:

$$\begin{aligned} F_{\Delta\pi}^{V(L)\rightarrow\gamma\pi}(q^2, p_\pi^2) &= F_{\nabla\pi}^{V(L)\rightarrow\gamma\pi}(q^2, p_\pi^2) \\ &= \int_{4m^2}^{\infty} \frac{ds}{\pi} \int_{4m^2}^{\infty} \frac{ds'}{\pi} \frac{\text{disc}_s \text{disc}_{s'} F_{\Delta\pi}^{V(L)\rightarrow\gamma\pi}(s', p_\pi^2)}{(s - M_{V(L)}^2)(s' - q^2)}. \end{aligned} \quad (61)$$

As in (39), we assume that the convergence of (61) is guaranteed by the vertices  $G_{V(L)}(s)$  and  $G_\gamma(s')$ .

Furthermore, we consider the production of photon,  $q^2 = 0$ , and use the photon wave function  $\psi_\gamma(s') = G_\gamma(s')/s'$ . After integrating over intermediate-state quark momenta, one can represent (61) for  $p_\pi^2 \leq 0$  in the following form:

$$\begin{aligned} F_{\Delta\pi}^{V(L)\rightarrow\gamma\pi}(0, p_\pi^2) &= F_{\nabla\pi}^{V(L)\rightarrow\gamma\pi}(0, p_\pi^2) \\ &= g_\pi \int_{4m^2}^{\infty} \frac{ds ds'}{16\pi^2} \psi_{V(L)}(s) \psi_\gamma(s') \\ &\times \frac{\Theta(-ss'p_\pi^2 - m^2\lambda(s, s', p_\pi^2))}{\sqrt{\lambda(s, s', p_\pi^2)}} S_{\Delta\pi}^{V(L)\rightarrow\gamma\pi}(s, s', p_\pi^2). \end{aligned} \quad (62)$$

The step-function  $\Theta(X)$  was defined in (41).

Let us emphasise once again that Eq. (62) is valid in the region  $p_\pi^2 \leq 0$  only. To obtain form factors at  $p_\pi^2 = M_\pi^2$ , one needs to continue Eq. (62) to the region  $p_\pi^2 > 0$ . Since the form factors are analytical functions in the vicinity of  $p_\pi^2 = 0$ , the straightforward way is to expand them in a series over  $p_\pi^2$  keeping constant and linear terms only:

$$F_{\Delta\pi}^{V(L)\rightarrow\gamma\pi}(0, p_\pi^2) = F_{\Delta\pi}^{V(L)\rightarrow\gamma\pi}(0, 0) + p_\pi^2 \frac{d}{dp_\pi^2} F_{\Delta\pi}^{V(L)\rightarrow\gamma\pi}(0, 0). \quad (63)$$

One can approximate  $p_\pi^2 \cdot F_{\Delta\pi}^{V(L)\rightarrow\gamma\pi}(0,0)/dp_\pi^2 = F_{\Delta\pi}^{V(L)\rightarrow\gamma\pi}(0,0) - F_{\Delta\pi}^{V(L)\rightarrow\gamma\pi}(0,-M_\pi^2)$  (here  $p_\pi^2 = -M_\pi^2$ ). Then

$$\begin{aligned} F_{\Delta\pi}^{V(L)\rightarrow\gamma\pi}(0, M_\pi^2) &= F_{\nabla\pi}^{V(L)\rightarrow\gamma\pi}(0, M_\pi^2) \\ &= 2F_{\Delta\pi}^{V(L)\rightarrow\gamma\pi}(0,0) - F_{\Delta\pi}^{V(L)\rightarrow\gamma\pi}(0, -M_\pi^2). \end{aligned} \quad (64)$$

Both form factors,  $F_{\Delta\pi}^{V(L)\rightarrow\gamma\pi}(0,0)$  and  $F_{\Delta\pi}^{V(L)\rightarrow\gamma\pi}(0, -M_\pi^2)$ , are calculated according to Eq. (62).

**3.0.9.  $Z$ -factors for pion emission** The charge factors for the pion emission in the decays  $\rho^+ \rightarrow \gamma\pi^+$ ,  $\rho^0 \rightarrow \gamma\pi^0$ ,  $\omega \rightarrow \gamma\pi^0$  (see Figs. 6, 7) are equal to those for photon emission as follows:

$$\begin{aligned} Z_{\Delta\pi}^{\rho^+ \rightarrow \gamma\pi^+} &= Z_{\nabla\gamma}^{\rho^+ \rightarrow \gamma\pi^+} = e_d, & Z_{\Delta\pi}^{\rho^+ \rightarrow \gamma\pi^+} &= Z_{\Delta\gamma}^{\rho^+ \rightarrow \gamma\pi^+} = e_u, \\ Z_{\Delta\pi}^{\rho^0 \rightarrow \gamma\pi^0} &= Z_{\nabla\pi}^{\rho^0 \rightarrow \gamma\pi^0} = Z_{\Delta\gamma}^{\rho^0 \rightarrow \gamma\pi^0} = Z_{\nabla\gamma}^{\rho^0 \rightarrow \gamma\pi^0} = \frac{1}{2}(e_u + e_d), \\ Z_{\Delta\pi}^{\omega \rightarrow \gamma\pi^0} &= Z_{\nabla\pi}^{\omega \rightarrow \gamma\pi^0} = Z_{\Delta\gamma}^{\omega \rightarrow \gamma\pi^0} = Z_{\nabla\gamma}^{\omega \rightarrow \gamma\pi^0} = \frac{1}{2}(e_u - e_d). \end{aligned} \quad (65)$$

In the calculation of  $Z$ -factors (65), we take into account that pion emission by quark is a two-step process (see Fig. 6c): the initial quark (for example, in Fig. 6a) emits gluons (they have isospin  $I_{gluons} = 0$ ) which produce quark-antiquark pairs,  $u\bar{u}$  or  $d\bar{d}$ , with equal amplitudes, and then we face the transition  $u\bar{d} \rightarrow \pi^+$ . The block of Fig. 6c is denoted as a coupling  $g_\pi$ .

In the process of Fig. 7a, the gluons produce  $u\bar{u}$  pair with the same amplitude as in the previous case but then we face the transition  $u\bar{u} \rightarrow \pi^0$  resulting in the factor  $1/\sqrt{2}$  (recall that  $\pi^0 = (u\bar{u} - d\bar{d})/\sqrt{2}$ ). In the process of Fig. 7c, the  $d\bar{d}$  pair is produced, and the transition  $d\bar{d} \rightarrow \pi^0$  gives the factor  $-1/\sqrt{2}$  (for more detailed presentation of the quark combinatorial rules see [2] and references therein).

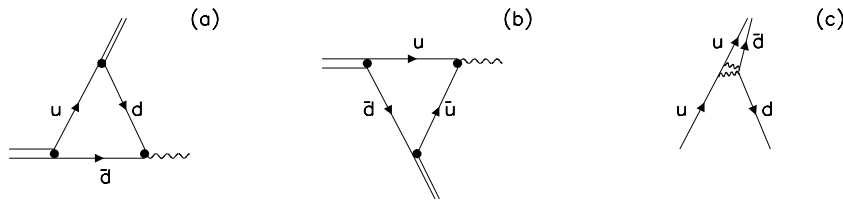


**Figure 6.** Diagrams for  $Z$ -factors in the reaction  $\rho^+ \rightarrow \gamma\pi^+$ : a)  $Z = e_d = -\frac{1}{3}$  and b)  $Z = e_u = \frac{2}{3}$ .

**3.0.10. Partial width** In terms of the calculated form factors, the partial width reads:

$$\begin{aligned} M_V \Gamma_{V \rightarrow \gamma\pi} &= \frac{1}{3} \cdot \frac{\alpha M_V^2 - M_\pi^2}{4 M_V^2} \frac{\lambda(M_V^2, M_\pi^2, 0)}{2} \\ &\times \left[ Z_{\Delta\gamma}^{V \rightarrow \gamma\pi} F_{\Delta\gamma}^{V \rightarrow \gamma\pi}(0, M_\pi^2) + Z_{\Delta\pi}^{V \rightarrow \gamma\pi} F_{\Delta\pi}^{V \rightarrow \gamma\pi}(0, M_\pi^2) \right. \\ &\quad \left. + Z_{\nabla\gamma}^{V \rightarrow \gamma\pi} F_{\nabla\gamma}^{V \rightarrow \gamma\pi}(0, M_\pi^2) + Z_{\nabla\pi}^{V \rightarrow \gamma\pi} F_{\nabla\pi}^{V \rightarrow \gamma\pi}(0, M_\pi^2) \right]^2. \end{aligned} \quad (66)$$

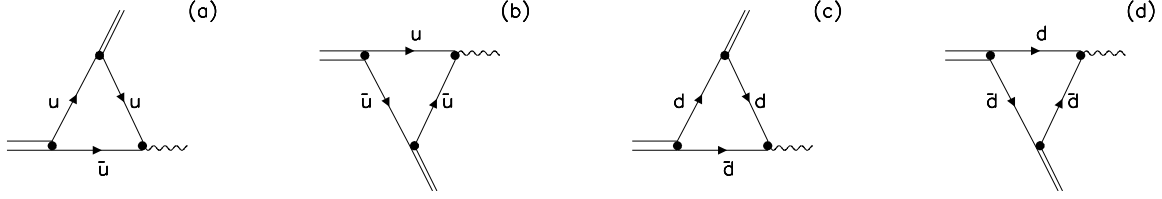


**Figure 7.** Diagrams for  $Z$ -factors in the reactions  $\rho^0 \rightarrow \gamma\pi^0$  and  $\omega^0 \rightarrow \gamma\pi^0$ : a)  $Z(\rho^0 \rightarrow \gamma\pi^0) = \frac{1}{3}$ ,  $Z(\omega \rightarrow \gamma\pi^0) = \frac{1}{3}$ ; b)  $Z(\rho^0 \rightarrow \gamma\pi^0) = \frac{1}{3}$ ,  $Z(\omega^0 \rightarrow \gamma\pi^0) = \frac{1}{3}$ ; c)  $Z(\rho^0 \rightarrow \gamma\pi^0) = -\frac{1}{6}$ ,  $Z(\omega^0 \rightarrow \gamma\pi^0) = \frac{1}{6}$ ; d)  $Z(\rho^0 \rightarrow \gamma\pi^0) = -\frac{1}{6}$ ,  $Z(\omega^0 \rightarrow \gamma\pi^0) = \frac{1}{6}$ . Recall that  $\rho^0 = \pi^0 = \frac{u\bar{u}-d\bar{d}}{\sqrt{2}}$ , and  $\omega^0 = \frac{u\bar{u}+d\bar{d}}{\sqrt{2}}$ .

Here, the factor  $1/3$  is due to the averaging over initial vector meson spin states, the term

$\alpha/4 \cdot (M_V^2 - M_\pi^2)/M_V^2$  is given by the phase space integration, and  $\lambda(M_V^2, M_\pi^2, 0)/2 = (M_V^2 - M_\pi^2)^2/2$  is due to the spin factor (21). The  $Z$ -factors are as follows:

$$Z_{\Delta\gamma}^{\rho^0 \rightarrow \gamma\pi^0} = 1/6, Z_{\nabla\gamma}^{\rho^0 \rightarrow \gamma\pi^0} = 1/6, Z_{\Delta\pi^0}^{\rho^0 \rightarrow \gamma\pi^0} = 1/6, Z_{\nabla\pi^0}^{\rho^0 \rightarrow \gamma\pi^0} = 1/6,$$

$$Z_{\Delta\gamma}^{\omega \rightarrow \gamma\pi^0} = 1/2, Z_{\nabla\gamma}^{\omega \rightarrow \gamma\pi^0} = 1/2, Z_{\Delta\pi^0}^{\omega \rightarrow \gamma\pi^0} = 1/2, Z_{\nabla\pi^0}^{\omega \rightarrow \gamma\pi^0} = 1/2.$$

#### 4. Results and discussion

The fitting to the partial widths  $\Gamma_{\rho^\pm \rightarrow \gamma\pi^\pm}^{(exp)} = 68 \pm 30$  keV,  $\Gamma_{\rho^0 \rightarrow \gamma\pi^0}^{(exp)} = 77 \pm 28$  keV,  $\Gamma_{\omega \rightarrow \gamma\pi^0}^{(exp)} = 776 \pm 45$  keV leads to the following values of the pion emission coupling:

$$\begin{aligned} \text{Solution I :} & \quad 16.7 \pm 0.3 \begin{matrix} +0.1 \\ -2.3 \end{matrix}, \\ \text{Solution II :} & \quad -3.0 \pm 0.3 \begin{matrix} +2.1 \\ -0.1 \end{matrix}. \end{aligned} \quad (67)$$

In Eq. (67), we have included systematical errors ( $(+0.1/ - 2.3)$  for Solution I and  $(+2.1/ - 0.1)$  for Solution II) which are caused by the uncertainties of the fit of  $q\bar{q}$  wave functions in the spectral integral equation (see Section 1.2).

So, we have regions of positive and negative  $g_\pi$ . However, one should take into account that the sign of  $g_\pi$  in (67) is rather conventional: it depends on signs of wave functions of photon and mesons involved into calculation. Because of that, being precise, we should state that for  $g_\pi$  we determine absolute values only, see (12).

Solution I gives us the value of the of pion–nucleon coupling; recall that it is determined as a factor in the phenomenological Lagrangian:  $g_{\pi NN} \left( \bar{\psi}'_N (\vec{\tau} \vec{\varphi}_\pi) i\gamma_5 \psi_N \right)$ . It is in agreement with the results for pion–nucleon scattering  $g_{\pi NN}^2/4\pi \simeq 14$  [39, 40, 41]. Namely, dealing with pion–nucleon interaction in terms of the quark model, we use the Lagrangian:

$$\begin{aligned} g_{\pi qq} \left( \bar{\psi}'_q (\vec{\tau} \vec{\varphi}_\pi) i\gamma_5 \psi_q \right) &= \sqrt{2} g_{\pi qq} \varphi_{\pi^+}^+ \left( \bar{\psi}'_d i\gamma_5 \psi_u \right) + \text{other terms} \\ &= g_\pi \varphi_{\pi^+}^+ \left( \bar{\psi}'_d i\gamma_5 \psi_u \right) + \text{other terms}, \end{aligned} \quad (68)$$

that gives us  $\sqrt{2} g_{\pi qq} = g_\pi$ .

In Appendix A, using SU(6)-symmetry for nucleons, we demonstrate that  $g_{\pi NN} = (5/3)g_{\pi qq}$ . So, in terms of SU(6)-symmetry, we have:

$$g_{\pi NN} = \frac{5}{3\sqrt{2}}g_{\pi}. \quad (69)$$

We see that Solution I, being in agreement with data [39, 40, 41], gives us

$$g_{\pi NN}^2/(4\pi) = 22.2 \pm 0.8_{-5.0}^{+0.2}. \quad (70)$$

For Solution II, we have found  $0.03 \leq g_{\pi NN}^2/(4\pi) \leq 1$ , that is far from the experimental value.

#### 4.1. Predictions for excited vector states

For  $\rho^\pm(2S)$ ,  $\rho^0(2S)$  and  $\omega(2S)$  mesons, we have found the following partial widths (in keV units):

$$\begin{aligned} \Gamma(\rho_{2S}^\pm \rightarrow \gamma\pi) &\simeq 10 - 130, \\ \Gamma(\rho_{2S}^0 \rightarrow \gamma\pi) &\simeq 10 - 130, \\ \Gamma(\omega_{2S} \rightarrow \gamma\pi) &\simeq 60 - 1080. \end{aligned} \quad (71)$$

The other wave functions of highly excited states have too large uncertainties to provide us with reliable widths. This points to the necessity to carry out measurements of radiative processes with mesons in the region of large masses.

*Acknowledgement* We thank B.L. Birbrair for helpful remarks. This paper was supported by the RFFI grant 07-02-01196-a.

## Appendix A: Nucleon pion emission vertex in the SU(6) quark model

Here we derive the relations between couplings in phenomenological Lagrangian for pions and nucleons,  $g_{\pi NN}(\bar{\psi}'_N(\vec{\tau}\vec{\varphi}_\pi)i\gamma_5\psi_N)$ , and those for quarks,  $g_{\pi qq}(\bar{\psi}'_q(\vec{\tau}\vec{\varphi}_\pi)i\gamma_5\psi_q)$ . To be definite, we consider transitions  $p^\uparrow \rightarrow \pi^+ + n^\downarrow$  and  $u^\uparrow \rightarrow \pi^+ + d^\downarrow$ . We use the following SU(6) wave functions (see, for example, Appendix D in Ref. [44]):

$$\begin{aligned} \psi_p &\equiv p^\uparrow(q(1)q(2)q(3)) = \frac{\sqrt{2}}{3}(u^\uparrow u^\uparrow d^\downarrow + d^\downarrow u^\uparrow u^\uparrow + u^\uparrow d^\downarrow u^\uparrow) \\ &\quad - \frac{1}{3\sqrt{2}}(u^\uparrow u^\downarrow d^\uparrow + d^\uparrow u^\uparrow u^\downarrow + u^\downarrow d^\uparrow u^\uparrow + u^\downarrow u^\uparrow d^\uparrow + d^\uparrow u^\downarrow u^\uparrow + u^\uparrow d^\uparrow u^\downarrow), \\ \bar{\psi}_n &\equiv n^\downarrow(q(1)q(2)q(3)) = \frac{\sqrt{2}}{3}(d^\downarrow d^\downarrow u^\uparrow + u^\uparrow d^\downarrow d^\downarrow + d^\downarrow u^\uparrow d^\downarrow) \\ &\quad - \frac{1}{3\sqrt{2}}(d^\downarrow d^\uparrow u^\downarrow + u^\downarrow d^\downarrow d^\uparrow + d^\uparrow u^\downarrow d^\downarrow + d^\uparrow d^\downarrow u^\downarrow + u^\downarrow d^\uparrow d^\downarrow + d^\downarrow u^\downarrow d^\uparrow). \end{aligned} \quad (72)$$

Recall that for baryon quarks we use notation of the type  $d^\downarrow u^\downarrow d^\uparrow \equiv d^\downarrow(1)u^\downarrow(2)d^\uparrow(3)$ .

The isospin block reads:

$$(\vec{\tau}\vec{\varphi}_\pi) = \sqrt{2} \frac{\tau_1 + i\tau_2}{2} \frac{\varphi_\pi^{(1)} - i\varphi_\pi^{(2)}}{\sqrt{2}} + \sqrt{2} \frac{\tau_1 - i\tau_2}{2} \frac{\varphi_\pi^{(1)} + i\varphi_\pi^{(2)}}{\sqrt{2}} + \tau_3\varphi_\pi^{(3)}. \quad (73)$$

Transition  $p^\uparrow \rightarrow \pi^+ + n^\downarrow$  is given by the following terms in nucleon and quark spaces:

$$\begin{aligned} g_{\pi NN} \langle \pi^+ n^\downarrow | \sqrt{2} \frac{\tau_1 + i\tau_2}{2} \frac{\varphi_\pi^{(1)} - i\varphi_\pi^{(2)}}{\sqrt{2}} i\gamma_5 | p^\uparrow \rangle \\ = g_{\pi qq} \langle \pi^+ n^\downarrow (q(1)q(2)q(3)) | \sqrt{2} \\ \times \sum_{j=1,2,3} \frac{\tau_1(j) + i\tau_2(j)}{2} \frac{\varphi_\pi^{(1)} - i\varphi_\pi^{(2)}}{\sqrt{2}} i\gamma_5(j) | p^\uparrow (q(1)q(2)q(3)) \rangle, \end{aligned} \quad (74)$$

where  $\tau_1(j)$ ,  $\tau_2(j)$  and  $\gamma_5(j)$  act on  $q(j)$ .

In the non-relativistic limit, which we use for nucleons and constituent quarks,

$$i\gamma_5 \rightarrow (-i)(\vec{\sigma}\vec{q})$$

and direct calculations give:

$$g_{\pi NN} = g_{\pi qq} \cdot 3 \cdot \frac{5}{9}. \quad (75)$$

To simplify the calculations which lead to (75), one can fix the direction of photon momentum, for example,  $\vec{q} = (q_x, 0, 0)$  and then use  $(\vec{q}\vec{\sigma}(j)) \rightarrow q_x\sigma_1(j)$ .

- [1] A.V. Anisovich, V.V. Anisovich, V.N. Markov, M.A. Matveev, V.A. Nikonov and A.V. Sarantsev, J. Phys. G: Nucl. Part. Phys. **31**, 1537 (2005).
- [2] A.V. Anisovich, V.V. Anisovich, M.A. Matveev, V.A. Nikonov, J. Nyiri, A.V. Sarantsev, "Mesons and baryons: systematisation and methods of analysis", World Scientific, Singapore, 2008.
- [3] A.V. Anisovich, V.V. Anisovich, V.N. Markov, M.A. Matveev, and A. V. Sarantsev, Yad. Fiz. **67**, 794 (2004) [Phys. At. Nucl., **67**, 773 (2004)].
- [4] G.F. Chew and S. Mandelstam, Phys. Rev. **119**, 467 (1960).
- [5] V.V. Anisovich, L.G. Dakhno, M.A. Matveev, V.A. Nikonov and A.V. Sarantsev, Yad. Fiz. **70**, 68 (2007) [Phys. At. Nucl., **70**, 63 (2007)], hep-ph/0510410; Yad. Fiz. **70**, 392 (2007) [Phys. At. Nucl., **70**, 364 (2007)], hep-ph/0511005.
- [6] V.V. Anisovich, L.G. Dakhno, M.A. Matveev, V.A. Nikonov and A.V. Sarantsev, Yad. Fiz. **70**, 480 (2007) [Phys. At. Nucl., **70**, 450 (2007)], hep-ph/0511109.
- [7] V.V. Anisovich, "Partons and constituent quarks in soft processes" Proc. of the XIV PNPI Winter School, p. 3, Leningrad, 1979; V.V. Anisovich, M.N. Kobrinsky, J. Nyiri, Yu.M. Shabelski "Quark model and high energy collisions", World Scientific, Singapore, 1985.
- [8] G. Parisi and R. Petronzio, Phys. Lett. B **94**, 51 (1980); M. Consoli and J.H. Field, Phys. Rev. D **49**, 1293 (1994).
- [9] J.M. Cornwell and J. Papavassiliou, Phys. Rev. D **40**, 3474 (1989).
- [10] V.V. Anisovich, S.M. Gerasyuta, and A.V. Sarantsev, Int. J. Mod. Phys. A **6**, 2625 (1991).
- [11] D.B. Leinweber *et al.*, Phys. Rev. D **58**, 031501 (1998).
- [12] E. Salpeter and H.A. Bethe, Phys. Rev. **84**, 1232 (1951); E. Salpeter, Phys. Rev. **91**, 994 (1953).
- [13] G. Hulth and H. Snellman, Phys. Rev D **24**, 2978 (1981).
- [14] S. Godfrey and N. Isgur, Phys. Rev. D **32**, 189 (1985).
- [15] W. Lucha, F. Schöberl, and D. Gromes, Phys. Rep. **200**, 127 (1991).

- [16] R. Ricken, M. Koll, D. Merten, B.C. Metsch, and H.R. Petry, Eur. Phys. J. A **9**, 221 (2000).
- [17] D. Ebert, R.N. Faustov, and V.O. Galkin, Phys. Rev. D **67**, 014027 (2003).
- [18] J. Linde and H. Snellman, Nucl. Phys. A **619**, 346 (1997).
- [19] S.N. Münz, Nucl. Rhys. A **609**, 364 (1996).
- [20] S.N. Gupta, S.F. Radford, and W.W. Repko, Phys. Rev. D **54**, 2075 (1996).
- [21] G.A. Schuler, F.A Berends, and R. van Gulik, Nucl. Rhys. B **523**, 423 (1998).
- [22] H.-W. Huang, *et. al.* Phys. Rev. D **54**, 2123 (1996); D **56**, 368 (1997).
- [23] V.V. Anisovich, M.N. Kobrinsky, D.I. Melikhov, and A.V. Sarantsev, Nucl. Phys. A **544**, 747 (1992);  
A.V. Anisovich and V.A. Sadovnikova, Yad. Fiz. **55**, 2657 (1992); **57**, 75 (1994); Eur. Phys. J. A **2**, 199 (1998).
- [24] V.V. Anisovich, D.I. Melikhov, and V.A. Nikonov, Phys. Rev. D **52**, 5295 (1995).
- [25] A.V. Anisovich, V.V. Anisovich, and V.A. Nikonov, Eur. Phys. J. A **12**, 103 (2001).
- [26] A.V. Anisovich, V.V. Anisovich, V.N. Markov, and V.A. Nikonov, Yad. Fiz. **65**, 523 (2002) [Phys. At. Nucl. **65**, 497 (2002)].
- [27] A.V. Anisovich, V.V. Anisovich, M.A. Matveev, and V.A. Nikonov, Yad. Fiz. **66**, 946 (2003) [Phys. At. Nucl. **66**, 914 (2003)].
- [28] A.V. Anisovich, V.V. Anisovich, V.N. Markov, M.A. Matveev and A.V. Sarantsev, J. Phys. G: Nucl. Part. Phys. **28**, 15 (2002).
- [29] A.V. Anisovich, C.A. Baker, C.J. Batty *et al.*, Phys. Lett. B **449**, 114 (1999); B **452**, 173 (1999); B **452**, 180 (1999); B **452**, 187 (1999); B **472**, 168 (2000); B **476**, 15 (2000); B **477**, 19 (2000); B **491**, 40 (2000); B **491**, 47 (2000); B **496**, 145 (2000); B **507**, 23 (2001); B **508**, 6 (2001); B **513**, 281 (2001); B **517**, 261 (2001); B **517**, 273 (2001);  
Nucl. Phys. A **651**, 253 (1999); A **662**, 319 (2000); A **662**, 344 (2000).
- [30] D. Barberis *et al.* (WA 102 Collab.), Phys. Lett. B **471**, 440 (2000).
- [31] R.S. Longacre and S.J. Lindenbaum, Report BNL-72371-2004; Phys. Rev. D **70**, 094041 (2004).
- [32] V.A. Schegelsky, A.V. Sarantsev and V.A. Nikonov, A.V. Anisovich, Eur. Phys. J. A **27**, 207 (2006).
- [33] V.A. Schegelsky, A.V. Sarantsev, A.V. Anisovich and M.P. Levchenko, Eur. Phys. J. A **27**, 199 (2006).
- [34] D.V. Bugg, Phys. Rep. **397**, 257 (2004).
- [35] E. Klempt and A. Zaitsev, Phys. Rept. **454**, 1 (2007).
- [36] A.V. Anisovich, V.V. Anisovich, and A.V. Sarantsev, Phys. Rev. D **62**, 051502(R) (2000).
- [37] A.V. Anisovich, V.V. Anisovich, L.G. Dakhno, V.A. Nikonov, and V.A. Sarantsev, Yad. Fiz. **68**, 1892 (2005) [Phys. Atom. Nucl. **68**, 1830 (2005)].
- [38] V.V. Anisovich, D.I. Melikhov, V.A. Nikonov, Phys. Rev. D **55**, 2918 (1997).
- [39] V. Stoks, R. Timmermans, J.J. de Swart, Phys. Rev. C **47**, 512 (1993).
- [40] R.A. Arndt, I.I. Strakovsky and R.L. Workman, Phys. Rev. C **50**, 2731 (1994); ArXiv:nucl-th/9506005.
- [41] D.V. Bugg, R. Marchleidt, " $\pi NN$  coupling constant from  $NN$  elastic data between 210 800 MeV", preprint NUCL-TH-9404017 (1994).
- [42] A.V. Anisovich, V.V. Anisovich and V.A. Nikonov, Eur. Phys. J. A **12**, 103 (2001).
- [43] A.V. Anisovich, V.V. Anisovich, M.A. Matveev and V.A. Nikonov, Yad. Fiz. **66**, 946 (2003) [Phys. Atom. Nucl. **66**, 914 (2003)].
- [44] V.V. Anisovich, M.N. Kobrinsky, J. Nyiri, Yu.M. Shabelski "*Quark model and high energy collisions*", 2nd edition, World Scientific, Singapore, 2004.